




## Article

# Can Machine Learning Predict Running Kinematics Based on Upper Trunk GPS-Based IMU Acceleration? A Novel Method of Conducting Biomechanical Analysis in the Field Using Artificial Neural Networks

Michael Lawson <sup>1,2,\*</sup> , Roozbeh Naemi <sup>1,3,\*</sup> , Robert A. Needham <sup>1</sup> and Nachiappan Chockalingam <sup>1</sup> 

<sup>1</sup> School of Health Science and Wellbeing, Staffordshire University, Stoke-on-Trent ST4 2DE, UK; r.needham@staffs.ac.uk (R.A.N.); n.chockalingam@staffs.ac.uk (N.C.)

<sup>2</sup> Middlesbrough Football Club, Middlesbrough TS3 6RS, UK

<sup>3</sup> School of Health and Society, University of Salford, Greater Manchester M6 6PU, UK

\* Correspondence: michael.lawson@research.staffs.ac.uk (M.L.); r.naemi@salford.ac.uk (R.N.)

**Abstract:** This study aimed to investigate whether running kinematics can be accurately estimated through an artificial neural network (ANN) model containing GPS-based accelerometer variables and anthropometric data. Thirteen male participants with extensive running experience completed treadmill running trials at several speeds. Participants wore a GPS device containing a triaxial accelerometer, and running kinematics were captured by an 18-camera motion capture system for each trial. Multiple multilayer perceptron neural network models were constructed to estimate participants' 3D running kinematics. The models consisted of the following input variables: 3D peak accelerometer acceleration during foot stance (g), stance time (s), running speed (km/h), participant height (cm), leg length (cm), and mass (kg). Pearson's correlation coefficient ( $r$ ), root mean squared error (RMSE), and relative root mean squared error (rRMSE) showed that ANN models provide accurate estimations of joint/segment angles (mean rRMSE =  $13.0 \pm 4.3\%$ ) and peak segment velocities (mean rRMSE =  $22.1 \pm 14.7\%$ ) at key gait phases across foot stance. The highest accuracies were achieved for flexion/extension angles of the thorax, pelvis, and hip, and peak thigh flexion/extension and vertical velocities (rRMSE < 10%). The current findings offer sports science and medical practitioners working with this data a method of conducting field-based analyses of running kinematics using a single IMU.

**Keywords:** artificial intelligence; accelerometer/s; GPS; IMU; kinematics



**Citation:** Lawson, M.; Naemi, R.; Needham, R.A.; Chockalingam, N. Can Machine Learning Predict Running Kinematics Based on Upper Trunk GPS-Based IMU Acceleration? A Novel Method of Conducting Biomechanical Analysis in the Field Using Artificial Neural Networks. *Appl. Sci.* **2024**, *14*, 1730. <https://doi.org/10.3390/app14051730>

Academic Editor: Arkady Voloshin

Received: 22 January 2024

Revised: 18 February 2024

Accepted: 20 February 2024

Published: 21 February 2024



**Copyright:** © 2024 by the authors. Licensee MDPI, Basel, Switzerland. This article is an open access article distributed under the terms and conditions of the Creative Commons Attribution (CC BY) license (<https://creativecommons.org/licenses/by/4.0/>).

## 1. Introduction

In recent years, there has been an exploration of the use of inertial measurement units (IMUs) to estimate joint kinematics during walking and running [1–6]. Conducting biomechanical analysis in the field with IMUs allows sports science and medical practitioners to capture an individual's locomotion characteristics [7]. The use of IMUs allows for more frequent analysis and reduces cost/set-up time compared to lab-based analysis [7]. Traditionally, IMUs, such as accelerometers, have been employed to analyze the acceleration profiles of bodily segments [8–10]. This type of analysis indirectly measures walking/running kinematics to observe differences between individuals or changes under conditions [8–10]. However, with recent advances in data processing procedures, it is now possible to directly estimate joint kinematics in the field with IMUs [1–5].

Conventional models utilizing IMUs to estimate joint kinematics have been previously employed to analyze patients' walking kinematics. Analyses of patients rehabilitating from hip arthroplasty [11] and knee ligament reconstruction [12] were used to inform the long-term effects on patients' post-surgery functionality. These earlier models mount IMUs on the proximal/distal segments to the relevant joint and measure the IMU sensor

orientation relative to the inertial frame [13]. Lab-based pre-calibration is required to ensure accurate sensor–sensor alignment to the anatomical axes and measurement of segment geometry so that a joint orientation matrix can be calculated [13]. The IMUs are utilized to reconstruct a biomechanical model of the human body. The linear relationships between the sensor acceleration profiles are then used to estimate the joint kinematics [2,14,15].

Accuracy is an important aspect of such measurements. Integration of accelerometer, gyroscope, and magnetometer data with sensor fusion algorithms has shown root mean squared errors (RMSEs) of  $<3.6^\circ$  when estimating 3D lower limb joint angles in the lab [16]. However, concerns about using IMUs to measure segmental orientation have been previously stated when applying these systems in the field [13]. Magnetometers are employed to reduce drift errors in the gyroscope’s angular velocity data by “resetting” the sensor orientation. Nevertheless, magnetic disturbances in the field can affect the magnetometer’s reference coordinates and are thus not recommended for field base use [13,17]. Additionally, soft tissue motion can lead to misalignment of the IMU sensors [18]. This is a common issue when conducting longitudinal analysis and greatly reduces the accuracy of models that rely on the linear relationship between two aligned sensors [2]. As a result, there is a lack of research that has successfully implemented these methods in the field over longer periods [19]. Recent developments in advanced data processing procedures have overcome previous regression-based problems with sensor misalignment [2], leading to the renewal of the use of IMUs to obtain field-based predictions of joint kinematics [2].

One of the deep learning algorithms is the artificial neural network (ANN). This allows for greater predictive accuracy than linear regression-based models when non-linear relationships between independent (input) and dependent (output) variables exist [20]. ANNs consist of interconnected units (neurons) separated into three layers: input, hidden, and output. Each layer contains several neurons, which are connected and appropriately weighted, depending on the strength of the connection between neurons [20,21]. Each ANN consists of training and testing modules. In the training module, the model learns the relationship between variables and appropriately “weights” each connection, depending on the fitting of the data structure [20]. The testing module then tests the algorithm to analyze how accurately the model has predicted the output variable.

Several classes of ANNs have been employed in studies that have attempted to predict biomechanical parameters during locomotion. Among these classes, multilayer perceptron (MLP) networks have performed well when predicting joint kinematics during walking [1,3,5]. MLP networks are considered a simpler form of ANN; they are easy to train and often employed as the baseline ANN to compare newer models against [3]. MLPs have shown an rRMSE of  $<9\%$  for lower limb kinematics during walking [5]. However, this error has increased to  $\sim 34\%$  when analyzing knee moments during running-based tasks [6]. As a result, more complex ANNs (convolutional neural networks) have been developed, integrating musculoskeletal simulations into the training module to improve accuracy [22,23]. However, these models’ pre-calibration procedures are extensive and require access to a biomechanics lab. In principle, however, the observed increased accuracy highlights the value of utilizing additional biomechanical input variables in ANNs to predict joint kinematics.

Previous investigations utilizing IMUs and ANNs to predict joint kinematics have typically stemmed from a clinical background [1,4]. Their application within sports has yet to be explored. With team sports athletes, IMUs within global positioning systems (GPS) are commonly used to monitor athletes’ workloads along with GPS-derived variables such as distance and running speed [24,25]. The GPS devices are mounted at approximately the posterior aspect of the upper thoracic spine, and the IMUs capture the acceleration profile of the upper trunk segment. There is the potential to use a single GPS-based IMU to measure the running kinematics of a player in the field. Previous research from the author found that the acceleration peaks captured by the GPS-based IMU are significantly influenced by an individual’s running kinematics [26]. More specifically, the peak velocities of the segments during foot contact had, on average, a greater effect on the acceleration

peaks than joint/segment angles [26]. However, the accuracy of employing GPS-based IMU data to directly estimate the kinematic profiles of joints and segments remains unclear.

Athlete anthropometrics [27], stance time [28], and running speed [29,30] have also been shown to have a relationship with an athlete's running kinematics. These variables are accessible to practitioners working with team sports athletes. Anthropometric measurements are routinely collected during skinfold body composition assessments [31]. Running speed can be accurately measured with coordinate data derived from GPS devices [32]. Stance time can also be measured with GPS-based IMU data [24,26]. Considering these, it was hypothesized that including these variables in addition to the IMU data could potentially increase the accuracy of ANNs in predicting running kinematics.

Including accurate estimations of an individual's running kinematics using GPS-based IMUs can offer more detailed biomechanical analyses of their performance in the field. The capacity to utilize IMUs within GPS devices to conduct field-based biomechanical analysis offers a tool for tracking an athlete's progression during injury rehabilitation. Therefore, the present study aims to investigate whether running kinematics can be accurately estimated through an ANN model containing GPS-based accelerometer variables, running speed, and anthropometric data. This study intends to explore the predictive capabilities of data easily accessible to sports science and medical practitioners to conduct comprehensive biomechanical analyses in the field.

## 2. Materials and Methods

A series of ANNs were selected and trained to predict kinematic variables (Section 2.3) that were identified as influencing the acceleration profile of the GPS-based IMU [26]. Additional input variables, such as anthropometrics, stance time characteristics, and running speed (Section 2.2), were added to the dataset to strengthen the ANN's predictive capabilities. The Staffordshire University ethical committee granted ethical clearance for this testing procedure (Reference number: LAWSON-TAGBIB-RN, approval date: 13 June 2018).

### 2.1. Experimental Set-Up

Thirteen males (age:  $27 \pm 3.7$  years, height:  $1.81 \pm 0.06$  m, mass:  $82.7 \pm 6.2$  kg) were selected to participate in the present study. The inclusion criteria for being selected were that participants were experienced runners (20–40 km per week) and free from injuries during testing. All participants gave informed written consent before testing. A single testing session, comprising nine trials of treadmill running (1-degree inclination) for 40 s (per trial), was completed by each participant. Treadmill running speeds started at 10 km/h and increased at 1 km/h increments to 18 km/h. Each trial was captured using an 18-camera motion capture system (Vicon, Oxford, UK). Participants wore a standard-issue vest containing a GPS device (STATSports Apex, Newry, Northern Ireland, UK) with an embedded high-frequency triaxial accelerometer and were provided with standardized running shoes (Puma Anzarun, Herzogenaurach, Germany).

The standard issue vest positioned the GPS device around the posterior aspect of the thoracic spine. The embedded triaxial accelerometer sampling frequency was set to 100 Hz (standard manufacturer setting). The positioning of the device orientated the accelerometer axes to the following planes of motion: *y*-axis (vertical), *z*-axis (anterior/posterior) and *x*-axis (medial/lateral). Fifty-four infrared markers (14 mm) were attached to the participants, corresponding to the modified Istituto Ortopedico Rizzoli (IOR) marker set with five additional clusters attached to the left thigh, right thigh, left shank, right shank, and the posterior aspect of the GPS device [33–35]. Eighteen optical cameras (VICON MXT40, Oxford, UK) recorded the coordinate data of the infrared markers at 100 Hz [36].

Raw accelerometer and marker coordinate data were transferred from the respective software (STATSport APEX version-2.0 and Vicon Nexus version-2.12) to Visual 3D software version-2022 (C-Motion Inc., Germantown, MD, USA). Synchronization of accelerometer and motion capture data was conducted by an assistant "tapping" the GPS device at the

beginning of each running trial. The frame of the tap was established in each data set, and then ten consecutive gait cycles were selected for analysis following a 20-s ramp period.

## 2.2. Input Variables

Three types of input variables were included in the ANNs (GPS-based accelerometer, anthropometric and running speed) due to the relationships previously found with running kinematics [26–30]. Stance time characteristics and peak accelerations during foot stance were selected as the GPS-based accelerometer input variables. Instances of initial foot contact (IFC), midstance (MS), and terminal foot contact (TFC) were identified in the vertical acceleration profile [26], and the subsequent timings (s) between these events were calculated (stance time, IFC-MS time, MS-TFC time). The vertical (VT), anterior/posterior (AP), medial/lateral (ML), and resultant (RES) peak accelerations during foot stance were then calculated by identifying the largest value on each axis during this time frame. The averages of each accelerometer variable were calculated across the ten gait cycles. Participant height (cm), body mass (kg), and leg length (cm) (distance from the anterior superior iliac spine to the medial malleolus) were recorded prior to testing and included as anthropometric input variables. Running speed (km/h) was derived from the treadmill speed within each trial and was the running speed input variable.

## 2.3. Output Variables

A previous investigation highlighted joint/segment kinematics that had significant relationships with the peak accelerations of the GPS-based accelerometer at foot stance phases [26]. Therefore, these findings provided the basis for selecting the output variables within a series of ANNs. Joint/segment angles at IFC, MS and TFC, and peak segment velocities during the impact (IFC-MS) and propulsion (MS-TFC) subphases were calculated for all bodily joints/segments. Tables 1 and 2 describe the kinematics that were included as output variables. The averages of the output variables were calculated over the ten gait cycles for each trial.

**Table 1.** The joint/segment angles selected as output variables in the ANNs.

Joint/Segment	Plane of Motion	Foot Stance Events
Thorax	Flexion/Extension	IFC & MS
	Internal/External Rotation	IFC
Pelvis	Flexion/Extension	IFC & MS
	Adduction/Abduction	IFC
Hip	Flexion/Extension	IFC
Thigh	Flexion/Extension	TFC
Knee	Flexion/Extension	IFC
Shank	Adduction/Abduction	TFC
Ankle	Flexion/Extension & Internal/External Rotation	MS
Foot	Flexion/Extension	TFC

## 2.4. ANN Model

The MLP class of ANNs was chosen as the deep learning algorithm to test the predictive capabilities of the input variables using IBM SPSS Modeler software version-22 (IBM Corp., Armonk, NY, USA). The model contained a feedforward architecture and was set to default. In this type of network, the connections are unidirectional, and information can only pass from the input layer to the hidden layer [37]. A single hidden layer was employed, which automatically selected the most appropriate number of hidden layer units (minimum = 1, maximum = 50). This is recommended when using MLP ANNs to prevent

overloading of the model, which can occur with a large number of hidden layers [38]. The dataset was partitioned randomly into a ~70% testing sample and a ~30% training sample depending on the relative number of cases. The layers are linked by activation functions that multiply the sum of the values in each unit by their weight, and are then transferred to the succeeding layer [37]. The activation link functions selected were the hyperbolic tangent  $\gamma(c) = \tanh(c) = (e^c - e^{-c}) / (e^c + e^{-c})$  for the hidden layer and the identity  $\gamma(c) = c$  function for the output layer due to the presence of scale-dependent variables.

**Table 2.** Peak segment velocities selected as output variables in the ANNs.

Segment	Plane of Motion	Type of Velocity	Foot Stance Subphases
Thorax	Vertical	Linear	Impact & Propulsion
	Horizontal	Linear	Impact
	Lateral	Linear	Propulsion
Pelvis	Horizontal	Linear	Impact & Propulsion
	Internal/External Rotation	Angular	Impact
	Flexion/Extension, Adduction/Abduction & Internal/External Rotation	Angular	Propulsion
	Lateral	Linear	Propulsion
Thigh	Vertical	Linear	Impact & Propulsion
	Internal/External Rotation	Angular	Impact
	Flexion/Extension & Internal/External Rotation	Angular	Propulsion
Shank	Adduction/Abduction	Angular	Impact & Propulsion
	Internal/External Rotation	Angular	Propulsion
Foot	Adduction/Abduction	Angular	Impact
	Internal/External Rotation	Angular	Impact & Propulsion
	Horizontal & Lateral	Linear	Propulsion

A total of 49 ANNs were produced, and each output variable was tested separately. Each ANN consisted of all the input variables, except for the peak accelerometer accelerations. The axis of peak accelerometer accelerations chosen depended on the output variable that had previously displayed a relationship with that input variable [26]. Therefore, each ANN contained either the RES, VT, AP, or ML peak accelerometer accelerations.

### 2.5. Statistical Analysis

Descriptive statistics of the ANN were conducted to provide insights into the average sample size percentages of the training and testing modules and the average number of units within the hidden layer. The root mean squared error (RMSE) and relative root mean squared error (rRMSE) for each ANN were calculated and used to assess the accuracy of each model in the training and testing modules. Pearson's correlation coefficient ( $r$ ) was used to measure the agreement between ANN estimated output variables, categorized as weak ( $r \leq 0.35$ ), moderate ( $0.35 < r \leq 0.67$ ), strong ( $0.67 < r \leq 0.90$ ), and excellent ( $\geq 0.90$ ) [6]. Sensitivity analysis of the input variables was performed to determine the individual importance of the predictors in determining the neural network and to identify the most important input variable (MIIV). All statistical analyses were performed using SPSS software (IBM Corporation, Armonk, NY, USA).

### 3. Results

The average dataset partitions utilized within the ANNs were  $72.8\% \pm 4.1\%$  (training) and  $27.2\% \pm 4.1\%$  (testing), with  $4.1 \pm 1.5$  hidden units. Model summaries showed, on average, that the accuracies of the ANNs to estimate the output variables were greater for joint/segment angles (testing rRMSE =  $13.0\% \pm 4.3\%$ ,  $r = 0.95 \pm 0.03$ ) than for peak segment velocities (testing rRMSE =  $22.1\% \pm 14.7\%$ ,  $r = 0.91 \pm 0.07$ ) (Table 3). Mean correlation coefficients showed excellent estimations of both groups of output variables ( $r > 0.90$ ) (Table 3).

**Table 3.** Mean accuracy (RMSE, root-mean squared error; rRMSE, relative root-mean squared error;  $r$ , Pearson’s correlation coefficient) of the estimated outcome variables by group.

Output Variable Group	Training		Testing		$r$
	RMSE	rRMSE (%)	RMSE	rRMSE (%)	
Joint/Segment Angles (°)	$3.33 \pm 2.88$	$8.8 \pm 7.4$	$1.86 \pm 0.65$	$13.0 \pm 4.3$	$0.95 \pm 0.03$
Peak Segment Velocities (m/s)	$5.35 \pm 4.28$	$14.1 \pm 11.5$	$3.83 \pm 3.14$	$22.1 \pm 14.7$	$0.91 \pm 0.07$
All Variables	$4.52 \pm 3.87$	$12.0 \pm 10.3$	$3.03 \pm 2.62$	$18.4 \pm 12.4$	$0.93 \pm 0.06$

Joint angle estimations had the smallest range in rRMSE (4.1–20.5%), with thorax flexion/extension angle during MS being the most accurate (RMSE =  $0.65^\circ$ ; rRMSE = 4.1%;  $r = 0.98$ ) (Table 4). However, estimations of the flexion/extension peak angular velocity during propulsion (MS-TFC) had the greatest accuracy of all output variables (RMSE = 0.24 m/s; rRMSE = 2.2%;  $r = 0.9$ ) (Table 5), and performed better when the RES accelerometer peak acceleration was included over the AP. The five joint/segment angles that could be predicted with the highest accuracy were thorax flexion/extension at IFC (RMSE =  $0.93^\circ$ ; rRMSE = 7.6%;  $r = 0.98$ ; MIIV = height) and MS (RMSE =  $0.65^\circ$ ; rRMSE = 4.1%;  $r = 0.98$ ; MIIV = ACC Peak), pelvis flexion/extension at IFC (RMSE =  $1.82^\circ$ ; rRMSE = 9.6%;  $r = 0.95$ ; MIIV = height) and MS (RMSE =  $1.56^\circ$ ; rRMSE = 9.2%;  $r = 0.96$ ; MIIV = height), and hip flexion/extension at IFC (RMSE =  $2.26^\circ$ ; rRMSE = 9.9%;  $r = 0.96$ ; MIIV = L leg length) (Figure 1).

**Table 4.** Individual accuracy (RMSE, root-mean squared error; rRMSE, relative root-mean squared error;  $r$ , Pearson’s correlation coefficient) of the estimated joint/segment angles during testing.

Accelerometer Peak Accel Axis	Output Variable					
	Body Joint/Segment	Plane of Motion	Gait Phase	RMSE (°)	rRMSE (%)	$r$
RES	HIP	Flexion/Extension	IFC	2.26	9.9%	0.96
	KNEE	Flexion/Extension	IFC	2.47	19.3%	0.83
	THORAX	Flexion/Extension	IFC	0.93	7.6%	0.98
	THORAX	Internal/External Rotation	IFC	1.86	15.0%	0.92
	ANKLE	Flexion/Extension	MS	2.19	12.2%	0.96
	PELVIS	Flexion/Extension	MS	1.56	9.2%	0.96
ML	THORAX	Internal/External Rotation	IFC	1.46	11.6%	0.95
	ANKLE	Internal/External Rotation	MS	1.17	12.6%	0.95
	SHANK	Adduction/Abduction	TFC	2.47	10.9%	0.96
	THIGH	Flexion/Extension	TFC	3.27	15.8%	0.97
VT	HIP	Flexion/Extension	IFC	1.70	10.0%	0.97
	THORAX	Flexion/Extension	IFC	1.58	19.5%	0.94
	ANKLE	Flexion/Extension	MS	1.79	13.6%	0.96
	PELVIS	Flexion/Extension	MS	1.08	11.5%	0.98
	ANKLE	Internal/External Rotation	MS	1.87	15.4%	0.96
AP	PELVIS	Adduction/Abduction	IFC	2.10	12.7%	0.94
	PELVIS	Flexion/Extension	IFC	1.82	9.6%	0.95
	THORAX	Flexion/Extension	MS	0.65	4.1%	0.98
	ANKLE	Internal/External Rotation	MS	2.15	19.0%	0.93
	FOOT	Flexion/Extension	TFC	2.91	20.5%	0.92

**Table 5.** Individual accuracy (RMSE, root-mean squared error; rRMSE, relative root-mean squared error; r, Pearson’s correlation coefficient) of the estimated peak segment velocities during testing.

Accelerometer Peak Accel Axis	Output Variable					
	Body Segment	Plane of Motion	Gait Phase	RMSE (m/s)	rRMSE (%)	r
RES	SHANK	Adduction/Abduction	IFC-MS	1.88	12.2%	0.97
	PELVIS	Internal/External Rotation	IFC-MS	3.09	15.5%	0.91
	PELVIS	Anterior/Posterior	IFC-MS	1.32	10.8%	0.94
	SHANK	Adduction/Abduction	MS-TFC	4.93	44.9%	0.69
	PELVIS	Flexion/Extension	MS-TFC	2.99	20.7%	0.88
	THIGH	Flexion/Extension	MS-TFC	0.24	2.2%	0.99
	SHANK	Internal/External Rotation	MS-TFC	5.30	28.8%	0.91
	THORAX	Medial/Lateral	MS-TFC	2.43	15.6%	0.96
ML	FOOT	Adduction/Abduction	IFC-MS	5.29	29.3%	0.87
	SHANK	Adduction/Abduction	IFC-MS	2.57	13.5%	0.96
	FOOT	Internal/External Rotation	IFC-MS	2.89	18.4%	0.92
	PELVIS	Adduction/Abduction	MS-TFC	3.20	28.0%	0.89
	THIGH	Flexion/Extension	MS-TFC	0.61	5.3%	0.99
	FOOT	Internal/External Rotation	MS-TFC	10.07	31.0%	0.88
	THIGH	Internal/External Rotation	MS-TFC	6.30	27.0%	0.91
	PELVIS	Medial/Lateral	MS-TFC	6.73	19.8%	0.93
VT	PELVIS	Anterior/Posterior	IFC-MS	4.83	28.1%	0.87
	THORAX	Anterior/Posterior	IFC-MS	6.26	47.8%	0.85
	THIGH	Vertical	IFC-MS	5.71	27.2%	0.91
	THIGH	Flexion/Extension	MS-TFC	0.71	5.7%	0.98
	PELVIS	Anterior/Posterior	MS-TFC	2.75	17.4%	0.92
	THIGH	Vertical	MS-TFC	1.34	9.3%	0.91
	THORAX	Vertical	MS-TFC	2.76	18.0%	0.93
AP	THIGH	Internal/External Rotation	IFC-MS	2.06	13.2%	0.98
	THORAX	Anterior/Posterior	IFC-MS	4.88	48.5%	0.80
	THORAX	Vertical	IFC-MS	15.06	65.0%	0.82
	THIGH	Flexion/Extension	MS-TFC	0.52	4.4%	0.99
	FOOT	Anterior/Posterior	MS-TFC	3.18	20.4%	0.91
	FOOT	Medial/Lateral	MS-TFC	1.22	12.9%	0.95

Kinematic Estimations of ANNs (< 10% rRMSE)

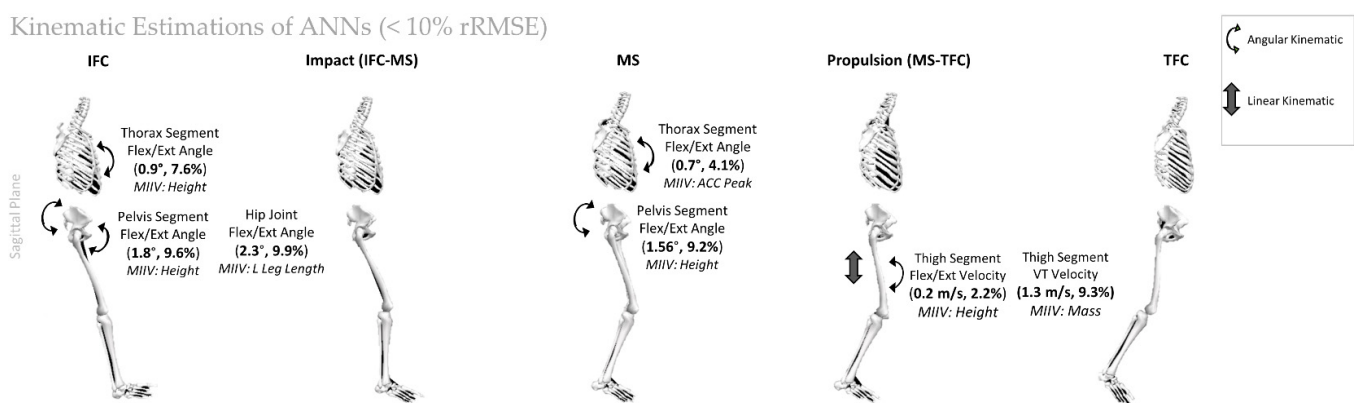


**Figure 1.** Output variables with rRMSE error of <10%. RMSE and rRMSE are displayed within the brackets of each variable. MIIV = the most important input variable from the sensitivity analysis.

Sensitivity analysis of the input variables showed that participant height (cm) had the highest average relative importance across estimations of joint angles (mean = 75% ± 25%) and was the most important variable in 7 ANNs (Figure 2), whereas the participant’s right leg length (cm) had the highest average relative importance across estimations of peak segment velocities (mean = 63% ± 29%) and was the most important in eight ANNs

(Figure 2). Peak accelerometer accelerations were ranked fourth (joint angles) and seventh (peak segment velocities) in average relative importance (Figures 2 and 3).

Estimation of joint/segment angles									
Output variable	Speed	ACC Peak	Height	Mass	LlegLength	RlegLength	StanceTime	IFC-MSTime	MS-TFCTime
1	44%	63%	73%	44%	100%	43%	24%	75%	37%
2	18%	65%	100%	49%	75%	74%	34%	79%	23%
3	32%	65%	100%	91%	27%	10%	43%	72%	75%
4	20%	16%	100%	82%	39%	35%	19%	41%	17%
5	29%	8%	74%	80%	65%	100%	35%	45%	48%
6	28%	29%	100%	38%	37%	25%	34%	29%	21%
7	19%	11%	100%	46%	46%	61%	15%	31%	22%
8	30%	58%	51%	100%	65%	80%	42%	91%	69%
9	24%	53%	100%	43%	25%	70%	8%	30%	5%
10	87%	41%	75%	31%	88%	100%	30%	66%	56%
11	43%	46%	61%	35%	100%	50%	37%	32%	41%
12	38%	61%	93%	91%	34%	57%	65%	100%	58%
13	46%	57%	25%	100%	95%	43%	19%	70%	40%
14	49%	100%	89%	56%	61%	31%	38%	36%	12%
15	36%	84%	60%	80%	84%	98%	13%	100%	72%
16	19%	54%	42%	54%	58%	100%	23%	65%	24%
17	27%	50%	100%	42%	57%	19%	21%	19%	25%
18	25%	100%	43%	23%	26%	23%	23%	29%	26%
19	36%	100%	76%	58%	42%	18%	32%	51%	68%
20	73%	96%	39%	100%	50%	54%	71%	74%	27%
Mean	36%	58%	75%	62%	59%	55%	31%	57%	38%
STDEV	18%	28%	25%	26%	25%	30%	16%	26%	21%

*Key: Output Variable Number) Accelerometer Peak Accel Axis-Body Segment-Plane of motion-Gait phase.*

(1) RES-HIP-Flex/Ext-IFC; (2) RES-KNEE-Flex/Ext-IFC; (3) RES-THORAX-Flex/Ext-IFC; (4) RES-THORAX-Int/Ext Rot-IFC; (5) RES-ANKLE-Flex/Ext-MS; (6) RES-PELVIS-Flex/Ext-MS; (7) ML-THORAX-Int/Ext Rot-IFC; (8) ML-ANKLE-Int/Ext Rot-MS; (9) ML-SHANK-Add/Abd-TFC; (10) ML-THIGH-Flex/Ext-TFC; (11) VT-HIP-Flex/Ext-IFC; (12) VT-THORAX-Flex/Ext-IFC; (13) VT-ANKLE-Flex/Ext-MS; (14) VT-PELVIS-Flex/Ext-MS; (15) VT-ANKLE-Int/Ext Rot-MS; (16) AP-PELVIS-Add/Abd-IFC; (17) AP-PELVIS-Flex/Ext-IFC; (18) AP-THORAX-Flex/Ext-MS; (19) AP-ANKLE-Int/Ext Rot-MS; (20) AP-FOOT-Flex/Ext-TFC

**Figure 2.** Matrix of relative importance for the input variables in the estimation of joint/segment angles. Speed = running speed (km/h); ACC peak = accelerometer peak acceleration (g); Height = participant height (cm); Mass = participant mass (kg); LLegLength = participant left leg length (cm); RLegLength = participant right leg length (cm); StanceTime = accelerometer derived stance time (s); IFC-MSTime = accelerometer derived time between IFC and MS; MS-TFCTime = accelerometer derived time between MS and TFC; STDEV = Standard deviation. The color scale represents the relative importance of each variable in the ANN: dark green = most important, light yellow = least important.



Estimation of peak segment velocities

Output variable	Speed	ACC Peak	Height	Mass	LlegLength	RlegLength	StanceTime	IFC-MSTime	MS-TFCTime
1	33%	74%	63%	100%	69%	61%	25%	25%	15%
2	52%	17%	21%	13%	63%	100%	21%	29%	11%
3	32%	26%	43%	62%	34%	48%	41%	100%	44%
4	80%	25%	100%	48%	79%	77%	46%	57%	27%
5	100%	5%	38%	19%	89%	56%	66%	68%	48%
6	49%	71%	100%	80%	61%	72%	58%	55%	92%
7	49%	63%	100%	60%	81%	49%	70%	57%	56%
8	67%	59%	59%	100%	45%	49%	48%	64%	67%
9	32%	23%	33%	80%	98%	100%	31%	85%	74%
10	42%	27%	89%	100%	70%	85%	23%	64%	27%
11	100%	5%	35%	18%	44%	21%	62%	50%	37%
12	32%	48%	35%	66%	55%	100%	62%	59%	31%
13	30%	15%	45%	18%	70%	100%	58%	35%	18%
14	100%	24%	9%	24%	12%	30%	24%	32%	19%
15	43%	55%	54%	77%	98%	100%	81%	90%	76%
16	100%	20%	30%	17%	74%	33%	24%	19%	17%
17	75%	49%	40%	100%	28%	100%	33%	60%	28%
18	38%	54%	79%	30%	95%	100%	27%	36%	29%
19	33%	14%	87%	41%	94%	100%	25%	59%	68%
20	53%	19%	30%	100%	28%	63%	28%	14%	14%
21	34%	20%	100%	31%	42%	48%	68%	34%	15%
22	81%	77%	74%	68%	100%	74%	19%	39%	53%
23	87%	44%	47%	28%	16%	44%	61%	43%	100%
24	100%	46%	50%	29%	60%	13%	33%	81%	47%
25	80%	92%	100%	98%	72%	19%	81%	97%	74%
26	35%	77%	100%	13%	41%	18%	63%	13%	21%
27	78%	67%	100%	43%	43%	60%	41%	48%	41%
28	39%	100%	42%	36%	53%	35%	52%	83%	45%
29	19%	100%	33%	49%	14%	59%	31%	28%	21%
<b>Mean</b>	<b>58%</b>	<b>45%</b>	<b>60%</b>	<b>53%</b>	<b>60%</b>	<b>63%</b>	<b>45%</b>	<b>53%</b>	<b>42%</b>
<b>STDEV</b>	<b>27%</b>	<b>29%</b>	<b>29%</b>	<b>31%</b>	<b>27%</b>	<b>29%</b>	<b>19%</b>	<b>25%</b>	<b>25%</b>

*Key: Output Variable Number) Accelerometer Peak Accel Axis-Body Segment-Plane of motion-Gait phase.*

(1) RES-SHANK-Add/Abd-IFC-MS; (2) RES-PELVIS-Int/Ext Rot-IFC-MS; (3) RES-SHANK-Add/Abd-MS-TFC; (4) RES-PELVIS-Flex/Ext-MS-TFC; (5) RES-THIGH-Flex/Ext-MS-TFC; (6) RES-SHANK-Int/Ext Rot-MS-TFC; (7) ML-FOOT-Add/Abd-IFC-MS; (8) ML-SHANK-Add/Abd-IFC-MS; (9) ML-FOOT-Int/Ext Rot-IFC-MS; (10) ML-PELVIS-Add/Abd-MS-TFC; (11) ML-THIGH-Flex/Ext-MS-TFC; (12) ML FOOT-Int/Ext Rot-MS-TFC; (13) ML-THIGH-Int/Ext Rot-MS-TFC; (14) VT-THIGH-Flex/Ext-MS-TFC; (15) VT-THIGH-Int/Ext Rot-IFC-MS; (16) VT-THIGH-Flex/Ext-MS-TFC; (17) RES-PELVIS-Horizontal-IFC-MS; (18) RES-THORAX-Lateral-MS-TFC; (19) ML-PELVIS-Lateral-MS-TFC; (20) VT-PELVIS-Horizontal-IFC-MS; (21) VT-THORAX-Horizontal-IFC-MS; (22) VT-THIGH-Vertical-IFC-MS; (23) VT-PELVIS-Horizontal-MS-TFC; (24) VT-THIGH-Vertical-MS-TFC; (25) VT-THORAX-Vertical-MS-TFC; (26) AP-THORAX-Horizontal-IFC-MS; (27) AP-THORAX-Vertical-IFC-MS; (28) AP-FOOT-Horizontal-MS-TFC; (29) AP-FOOT-Lateral-MS-TFC

**Figure 3.** Matrix of relative importance for the input variables in the estimation of peak segment velocities. Speed = running speed (km/h); ACC peak = accelerometer peak acceleration (g); Height = participant height (cm); Mass = participant mass (kg); LLegLength = participant left leg length (cm); RLegLength = participant right leg length (cm); StanceTime = accelerometer derived stance time (s); IFC-MSTime = accelerometer derived time between IFC and MS; MS-TFCTime = accelerometer derived time between MS and TFC; STDEV = Standard deviation. The color scale represents the relative importance of each variable in the ANN: dark green = most important, light yellow = least important.

#### 4. Discussion

This study aimed to determine the predictive capabilities of ANNs containing GPS-based accelerometer, running speed, and anthropometric data to estimate running kinematics. The study's results provide preliminary insights into the application of deep learning algorithms with data that are easily accessible to sports science and medical practitioners working with team sports athletes to conduct analyses of running kinematics in the field.

Correlation coefficients of the estimated vs. actual output variables ranged from strong to excellent across all output variables, showing that the model's performance was highly accurate. Overall, estimations of joint/segment angles (mean rRMSE =  $13.0 \pm 4.3\%$ ) were better than peak segment velocities (mean rRMSE =  $22.1 \pm 14.7\%$ ). Previous research [26] found that peak segment velocities had a greater effect on GPS-based accelerometer peak accelerations than joint/segment angles in linear regression-based analysis. Conversely, in the current study, better accuracy was observed in predicting joint/segment angles than in predicting peak segment velocities. This indicates a stronger relationship between the input variables and joint/segment angles. Including added input variables (running speed, stance times, anthropometrics) or the capability of ANNs to utilize non-linear relationships may be responsible for this finding.

Sensitivity analysis of the input variables highlighted that the GPS-based IMU variables were, on average, not the most important variables in both joint/segment and peak segment velocities estimations (Figures 2 and 3). However, the performance of each ANN must be considered. Accelerometer peak acceleration had the highest relative importance in estimating thorax flexion/extension at MS, which was the most accurate estimation of all joint/segment angles. Despite this, the value of including anthropometric input variables in ANNs has become evident in the current study. The input variables with the highest mean relative importance for joint/segment angles were participant height ( $75 \pm 25\%$ ) and mass ( $62 \pm 26\%$ ). For peak segment velocities, leg length (right =  $63 \pm 29\%$ ; left =  $60 \pm 27\%$ ) and height ( $60 \pm 29\%$ ) were the highest. Anthropometric data has been previously employed within the pre-calibration procedures of conventional neural networks to improve the accuracy of estimating joint kinematics [3]. Our results also show that anthropometric data can aid multilayer perceptron ANNs instead of relying on IMU data alone.

There were five joint angles (Hip flexion/extension at IFC; Thorax flexion/extension at IFC; Thorax flexion/extension at MS; Pelvis flexion/extension at IFC; Pelvis flexion/extension at MS) and two peak segment velocities (Thigh flexion/extension during propulsion; Thigh vertical during propulsion) that had rRMSEs of  $<10\%$  (Figure 1). Previous investigations have typically only analyzed lower limb kinematics and found hip flexion/extension RMSE values of  $5.1\text{--}5.6^\circ$  and knee flexion/extension RMSE values of  $4.8\text{--}6.5^\circ$  during running [22,23]. The present study differed from previous investigations, as estimations of joint/segment angles at specific gait events were estimated rather than the continuous joint angle over the whole gait cycle and the type of ANN used. Nevertheless, our results showed that the RMSE values of knee flexion/extension at IFC were  $2.47^\circ$ . It can be suggested that MLP ANNs could achieve similar or greater accuracy in estimating hip and knee sagittal joint angles than previous methods. These findings also highlight the importance of including anthropometric data, as they had the highest importance in four of the five most accurate variables (Figure 1). Accurate estimations of peak thigh flexion/extension and vertical velocities during propulsion were also observed (rRMSE  $\leq 9.3\%$ ). However, there are no previous studies against which to compare these results.

There are several practical applications of the present study's findings. Analyzing the sagittal plane kinematics of athletes in the field can provide sports science and medical practitioners with useful insights into their athletes' physical condition and running performance. Trunk flexion/extension angle has been shown to increase when localized muscular fatigue is present [39,40]. Additionally, more experienced runners typically have less trunk flexion and reduced peak hip flexion during foot contact, resulting in increased performance [41] and reduced injury risk [42]. Segment velocities can also be used to characterize performance, as thigh flexion/extension angular velocity has been shown to

be a determining factor during sprint running [43]. Our results showed that all of these variables could be accurately estimated with ANNs, thus providing practitioners with a method to quantify running performance and monitor fatigue in the field.

The findings of this study can also be used in relation to sports injury analysis. Accurate estimations of knee flexion/extension angle were found, which could be employed in connection with anterior cruciate ligament (ACL) injuries. Athletes who have undergone ACL reconstruction can limit knee extension during running for up to one-year post-surgery [44]. Therefore, monitoring this variable during rehabilitation can provide insights into an athlete's progress. It has also been suggested that athletes with limited knee flexion during running, jumping, and cutting tasks have a greater risk of suffering noncontact ACL injuries [45], which is prevalent among female athletes [46]. However, it must be stated that the current study analyzed only the prediction capabilities during straight-line, steady-state running. Whether the same accuracies in running kinematic estimation can be achieved in jumping and multidirectional tasks remains unclear. However, the present study offers the potential for practitioners to accurately measure sagittal plane kinematics that are of interest in hip and knee injuries.

Furthermore, the methodology employed in this study utilized commercially available software (IBM SPSS Modeler software version-22) to compute the MLP ANNs. Using this software does not require knowledge or experience in building and training ANNs. Most sports science and medicine university degrees teach the use of SPSS software during their research methods modules. Thus, the methodology used in the present study is reproducible by those sports science and medical practitioners who have undergone a university degree and can be introduced into their daily practices.

The limitations of the present study are that the output variables were specific to gait events. Analyzing joint/segment angles and velocities over the whole gait cycle would provide a more comprehensive insight into the capacity of ANNs to predict running kinematics with data from GPS devices and anthropometric measurements. Additionally, MLPs are a simple form of ANN, and greater accuracy may be achieved with more complex classes of ANNs [3].

Moreover, the present study used a small number of participants. Considering the high accuracies reported here, increasing the sample size would allow for more data to train the ANN model and lead to potentially stronger predictions. Future research could explore this concept and aim to estimate kinematics over the whole gait cycle instead of specific time events. In addition, including multidirectional running would allow for kinematic analysis of the more sports-specific movement tasks that athletes complete in the field.

## 5. Conclusions

The present study showed that running kinematics can be predicted with ANNs consisting of GPS-based IMU, treadmill-derived running speed, and anthropometric data. Accurate estimations of sagittal plane joint/segment angles and peak segment velocities were achieved. The highest estimation accuracy was found for flexion/extension angles of the thorax, pelvis and hip, and peak thigh flexion/extension and vertical velocities. Our findings offer sports science and medical practitioners working with this data a method of conducting field-based analyses of running kinematics. The proposed method could have practical implications for measuring biomechanical variables associated with performance and injury rehabilitation in the field.

**Author Contributions:** The contributions by the authors are as follows: Conceptualization, M.L., R.A.N., R.N. and N.C.; Methodology, M.L. and R.N.; Software, M.L. and R.A.N.; Formal Analysis, M.L., R.N. and R.A.N.; Writing—Original Draft Preparation, M.L. and R.N.; Writing—Reviewing and Editing, R.A.N., R.N. and N.C.; Visualization, M.L.; Supervision, R.N. and N.C. All authors have read and agreed to the published version of the manuscript.

**Funding:** This research received no external funding.

**Institutional Review Board Statement:** Ethical clearance for this testing procedure was granted by the Staffordshire University ethical committee (Reference number: LAWSON-TAGBIB-RN, approval date: 13 June 2018).

**Informed Consent Statement:** All participants gave informed written consent prior to testing.

**Data Availability Statement:** The original contributions presented in the study are included in the article, further inquiries can be directed to the corresponding authors.

**Conflicts of Interest:** Author M.L. was employed by the company Middlesbrough Football Club. The remaining authors declare that the research was conducted in the absence of any commercial or financial relationship that could be construed as a potential conflict of interest.

## References

- Mundt, M.; Thomsen, W.; Witter, T.; Koeppe, A.; David, S.; Bamer, F.; Potthast, W.; Markert, B. Prediction of Lower Limb Joint Angles and Moments during Gait Using Artificial Neural Networks. *Med. Biol. Eng. Comput.* **2020**, *58*, 211–225. [[CrossRef](#)]
- Zimmermann, T.; Taetz, B.; Bleser, G. IMU-to-Segment Assignment and Orientation Alignment for the Lower Body Using Deep Learning. *Sensors* **2018**, *18*, 302. [[CrossRef](#)] [[PubMed](#)]
- Mundt, M.; Johnson, W.R.; Potthast, W.; Markert, B.; Mian, A.; Alderson, J. A Comparison of Three Neural Network Approaches for Estimating Joint Angles and Moments from Inertial Measurement Units. *Sensors* **2021**, *21*, 4535. [[CrossRef](#)]
- Rapp, E.; Shin, S.; Thomsen, W.; Ferber, R.; Halilaj, E. Estimation of Kinematics from Inertial Measurement Units Using a Combined Deep Learning and Optimization Framework. *J. Biomech.* **2021**, *116*, 110229. [[CrossRef](#)] [[PubMed](#)]
- Lim, H.; Kim, B.; Park, S. Prediction of Lower Limb Kinetics and Kinematics during Walking by a Single IMU on the Lower Back Using Machine Learning. *Sensors* **2019**, *20*, 130. [[CrossRef](#)] [[PubMed](#)]
- Stetter, B.J.; Krafft, F.C.; Ringhof, S.; Stein, T.; Sell, S. A Machine Learning and Wearable Sensor Based Approach to Estimate External Knee Flexion and Adduction Moments During Various Locomotion Tasks. *Front. Bioeng. Biotechnol.* **2020**, *8*, 9. [[CrossRef](#)] [[PubMed](#)]
- Cronin, N.J. Using Deep Neural Networks for Kinematic Analysis: Challenges and Opportunities. *J. Biomech.* **2021**, *123*, 110460. [[CrossRef](#)] [[PubMed](#)]
- Sinclair, J.; Hobbs, S.J.; Protheroe, L.; Edmundson, C.J.; Greenhalgh, A. Determination of Gait Events Using an Externally Mounted Shank Accelerometer. *J. Appl. Biomech.* **2013**, *29*, 118–122. [[CrossRef](#)]
- Lindsay, T.R.; Yaggie, J.A.; McGregor, S.J. Contributions of Lower Extremity Kinematics to Trunk Accelerations during Moderate Treadmill Running. *J. Neuroeng. Rehabil.* **2014**, *11*, 162. [[CrossRef](#)]
- Boutayayamou, M.; Schwartz, C.; Stamatakis, J.; Denoël, V.; Maquet, D.; Forthomme, B.; Croisier, J.L.; Macq, B.; Verly, J.G.; Garraux, G.; et al. Development and Validation of an Accelerometer-Based Method for Quantifying Gait Events. *Med. Eng. Phys.* **2015**, *37*, 226–232. [[CrossRef](#)]
- Zijlstra, A.; Goosen, J.H.M.; Verheyen, C.C.P.M.; Zijlstra, W. A Body-Fixed-Sensor Based Analysis of Compensatory Trunk Movements during Unconstrained Walking. *Gait Posture* **2008**, *27*, 164–167. [[CrossRef](#)]
- Favre, J.; Luthi, F.; Jolles, B.M.; Siegrist, O.; Najafi, B.; Aminian, K. A New Ambulatory System for Comparative Evaluation of the Three-Dimensional Knee Kinematics, Applied to Anterior Cruciate Ligament Injuries. *Knee Surg. Sport. Traumatol. Arthrosc.* **2006**, *14*, 592–604. [[CrossRef](#)]
- Picerno, P. 25 Years of Lower Limb Joint Kinematics by Using Inertial and Magnetic Sensors: A Review of Methodological Approaches. *Gait Posture* **2017**, *51*, 239–246. [[CrossRef](#)]
- Willemsen, A.T.M.; van Alsté, J.A.; Boom, H.B.K. Real-Time Gait Assessment Utilizing a New Way of Accelerometry. *J. Biomech.* **1990**, *23*, 859–863. [[CrossRef](#)]
- Dejnabadi, H.; Jolles, B.M.; Aminian, K. A New Approach to Accurate Measurement of Uniaxial Joint Angles Based on a Combination of Accelerometers and Gyroscopes. *IEEE Trans. Biomed. Eng.* **2005**, *52*, 1478–1484. [[CrossRef](#)]
- Picerno, P.; Cereatti, A.; Cappozzo, A. Joint Kinematics Estimate Using Wearable Inertial and Magnetic Sensing Modules. *Gait Posture* **2008**, *28*, 588–595. [[CrossRef](#)]
- Picerno, P.; Cereatti, A.; Cappozzo, A. A Spot Check for Assessing Static Orientation Consistency of Inertial and Magnetic Sensing Units. *Gait Posture* **2011**, *33*, 373–378. [[CrossRef](#)]
- Frick, E.; Rahmatalla, S. Joint Center Estimation Using Single-Frame Optimization: Part 2: Experimentation. *Sensors* **2018**, *18*, 2563. [[CrossRef](#)]
- Weygers, I.; Kok, M.; Konings, M.; Hallez, H.; De Vroey, H.; Claeys, K. Inertial Sensor-Based Lower Limb Joint Kinematics: A Methodological Systematic Review. *Sensors* **2020**, *20*, 673. [[CrossRef](#)]
- Aryadoust, V.; Goh, C.C. Predicting Listening Item Difficulty with Language Complexity Measures: A Comparative Data Mining Study. *CaMLA Work. Pap.* **2014**, *2*, 1–16.
- Barbour, B.; Brunel, N.; Hakim, V.; Nadal, J.-P. What Can We Learn from Synaptic Weight Distributions? *Trends Neurosci.* **2007**, *30*, 622–629. [[CrossRef](#)]

22. Dorschky, E.; Nitschke, M.; Martindale, C.F.; van den Bogert, A.J.; Koelewijn, A.D.; Eskofier, B.M. CNN-Based Estimation of Sagittal Plane Walking and Running Biomechanics from Measured and Simulated Inertial Sensor Data. *Front. Bioeng. Biotechnol.* **2020**, *8*, 604. [[CrossRef](#)]
23. Gholami, M.; Rezaei, A.; Cuthbert, T.J.; Napier, C.; Menon, C. Lower Body Kinematics Monitoring in Running Using Fabric-Based Wearable Sensors and Deep Convolutional Neural Networks. *Sensors* **2019**, *19*, 5325. [[CrossRef](#)]
24. Buchheit, M.; Gray, A.; Morin, J.-B.B. Assessing Stride Variables and Vertical Stiffness with GPS-Embedded Accelerometers: Preliminary Insights for the Monitoring of Neuromuscular Fatigue on the Field. *J. Sports Sci. Med.* **2015**, *14*, 698–701.
25. Barrett, S.; Midgley, A.; Lovell, R. PlayerLoad™: Reliability, Convergent Validity, and Influence of Unit Position during Treadmill Running. *Int. J. Sports Physiol. Perform.* **2014**, *9*, 945–952. [[CrossRef](#)]
26. Lawson, M.; Naemi, R.; Needham, R.A.; Chockalingam, N. The Effects of Running Kinematics on Peak Upper Trunk GPS-Measured Accelerations during Foot Contact at Different Running Speeds. *Appl. Sci.* **2023**, *14*, 63. [[CrossRef](#)]
27. Black, M.I.; Allen, S.J.; Forrester, S.E.; Folland, J.P. The Anthropometry of Economical Running. *Med. Sci. Sport. Exerc.* **2020**, *52*, 762–770. [[CrossRef](#)]
28. De Wit, B.; De Clercq, D.; Aerts, P. Biomechanical Analysis of the Stance Phase during Barefoot and Shod Running. *J. Biomech.* **2000**, *33*, 269–278. [[CrossRef](#)]
29. Fukuchi, R.K.; Fukuchi, C.A.; Duarte, M. A Public Dataset of Running Biomechanics and the Effects of Running Speed on Lower Extremity Kinematics and Kinetics. *PeerJ* **2017**, *5*, e3298. [[CrossRef](#)]
30. Brughelli, M.; Cronin, J.; Chaouachi, A. Effects of Running Velocity on Running Kinetics and Kinematics. *J. Strength Cond. Res.* **2011**, *25*, 933–939. [[CrossRef](#)]
31. Bernal-Orozco, M.F.; Posada-Falomir, M.; Quiñónez-Gastélum, C.M.; Plascencia-Aguilera, L.P.; Arana-Nuño, J.R.; Badillo-Camacho, N.; Márquez-Sandoval, F.; Holway, F.E.; Vizmanos-Lamotte, B. Anthropometric and Body Composition Profile of Young Professional Soccer Players. *J. Strength Cond. Res.* **2020**, *34*, 1911–1923. [[CrossRef](#)]
32. Varley, M.C.; Fairweather, I.H.; Aughey, R.J. Validity and Reliability of GPS for Measuring Instantaneous Velocity during Acceleration, Deceleration, and Constant Motion. *J. Sports Sci.* **2012**, *30*, 121–127. [[CrossRef](#)]
33. Leardini, A.; Sawacha, Z.; Paolini, G.; Inghrosso, S.; Nativio, R.; Benedetti, M.G. A New Anatomically Based Protocol for Gait Analysis in Children. *Gait Posture* **2007**, *26*, 560–571. [[CrossRef](#)]
34. Leardini, A.; Biagi, F.; Merlo, A.; Belvedere, C.; Benedetti, M.G. Multi-Segment Trunk Kinematics during Locomotion and Elementary Exercises. *Clin. Biomech.* **2011**, *26*, 562–571. [[CrossRef](#)]
35. Needham, R.; Naemi, R.; Healy, A.; Chockalingam, N. Multi-Segment Kinematic Model to Assess Three-Dimensional Movement of the Spine and Back during Gait. *Prosthetics Orthot. Int.* **2016**, *40*, 624–635. [[CrossRef](#)] [[PubMed](#)]
36. Merriault, P.; Dupuis, Y.; Boutteau, R.; Vasseur, P.; Savatier, X. A Study of Vicon System Positioning Performance. *Sensors* **2017**, *17*, 1591. [[CrossRef](#)]
37. Jiang, J.; Trundle, P.; Ren, J. Medical Image Analysis with Artificial Neural Networks. *Comput. Med. Imaging Graph.* **2010**, *34*, 617–631. [[CrossRef](#)]
38. Marius-Constantin, P.; Balas, V.E.; Perescu-Popescu, L.; Mastorakis, N. Multilayer Perceptron and Neural Networks. *WSEAS Trans. Circuits Syst.* **2009**, *8*, 579–588.
39. Hart, J.M.; Kerrigan, D.C.; Fritz, J.M.; Ingersoll, C.D. Jogging Kinematics After Lumbar Paraspinal Muscle Fatigue. *J. Athl. Train.* **2009**, *44*, 475–481. [[CrossRef](#)]
40. Strohrmann, C.; Harms, H.; Kappeler-setz, C.; Tröster, G. Monitoring Kinematic changes with Fatigue in Running Using Body-Worn Sensors. *IEEE Trans. Inf. Technol. Biomed.* **2012**, *16*, 983–990. [[CrossRef](#)]
41. Folland, J.P.; Allen, S.J.; Black, M.I.; Handsaker, J.C.; Forrester, S.E. Running Technique Is an Important Component of Running Economy and Performance. *Med. Sci. Sport. Exerc.* **2017**, *49*, 1412–1423. [[CrossRef](#)]
42. Quan, W.; Ren, F.; Sun, D.; Fekete, G.; He, Y. Do Novice Runners Show Greater Changes in Biomechanical Parameters? *Appl. Bionics Biomech.* **2021**, *2021*, 8894636. [[CrossRef](#)]
43. Hunter, J.P.; Marshall, R.N.; McNair, P.J. Segment-Interaction Analysis of the Stance Limb in Sprint Running. *J. Biomech.* **2004**, *37*, 1439–1446. [[CrossRef](#)]
44. Asaeda, M.; Deie, M.; Kono, Y.; Mikami, Y.; Kimura, H.; Adachi, N. The Relationship between Knee Muscle Strength and Knee Biomechanics during Running at 6 and 12 Months after Anterior Cruciate Ligament Reconstruction. *Asia-Pac. J. Sport. Med. Arthrosc. Rehabil. Technol.* **2019**, *16*, 14–18. [[CrossRef](#)]
45. Yu, B.; Garrett, W.E. Mechanisms of Non-Contact ACL Injuries. *Br. J. Sports Med.* **2007**, *41*, i47–i51. [[CrossRef](#)]
46. Malinzak, R.A.; Colby, S.M.; Kirkendall, D.T.; Yu, B.; Garrett, W.E. A Comparison of Knee Joint Motion Patterns between Men and Women in Selected Athletic Tasks. *Clin. Biomech.* **2001**, *16*, 438–445. [[CrossRef](#)]

**Disclaimer/Publisher's Note:** The statements, opinions and data contained in all publications are solely those of the individual author(s) and contributor(s) and not of MDPI and/or the editor(s). MDPI and/or the editor(s) disclaim responsibility for any injury to people or property resulting from any ideas, methods, instructions or products referred to in the content.